Supplement of Atmos. Chem. Phys., 23, 8583–8590, 2023
https://doi.org/10.5194/acp-23-8583-2023-supplement

Atmospheric Chemistry and Physics
Open Access

Supplement of

A new steady-state gas–particle partitioning model of polycyclic aromatic hydrocarbons: implication for the influence of the particulate proportion in emissions

Fu-Jie Zhu et al.

Correspondence to: Wan-Li Ma (mawanli002@163.com)

Contents

S1. Texts

Text S1. The introduction of the steady-state six-compartment six-fugacity model

Multimedia fugacity models have been used to address chemical pollution by providing a quantitative account of the sources, transport processes, fate and sinks of organic chemicals(Mackay, 2001). A steady-state six-compartment (gas, particle, liquid, suspended particle mater (SPMs), soil, sediments) six-fugacity model was derived using the fugacity theory (Li et al., 2021b). The six-compartment six-fugacity system was exhibited in following figure. The subscripts represent different environment matrix: gas (G), liquid (L), soil (S), sediment (Sed), particle in air (P), and particle in liquid (O). The primary equation in fugacity models is the relationship between the flux (F) and the fugacity (f):

$$F = fD \quad \text{(S1)}$$

where D is the intermedia D values defined in the fugacity theory(Mackay, 2001).

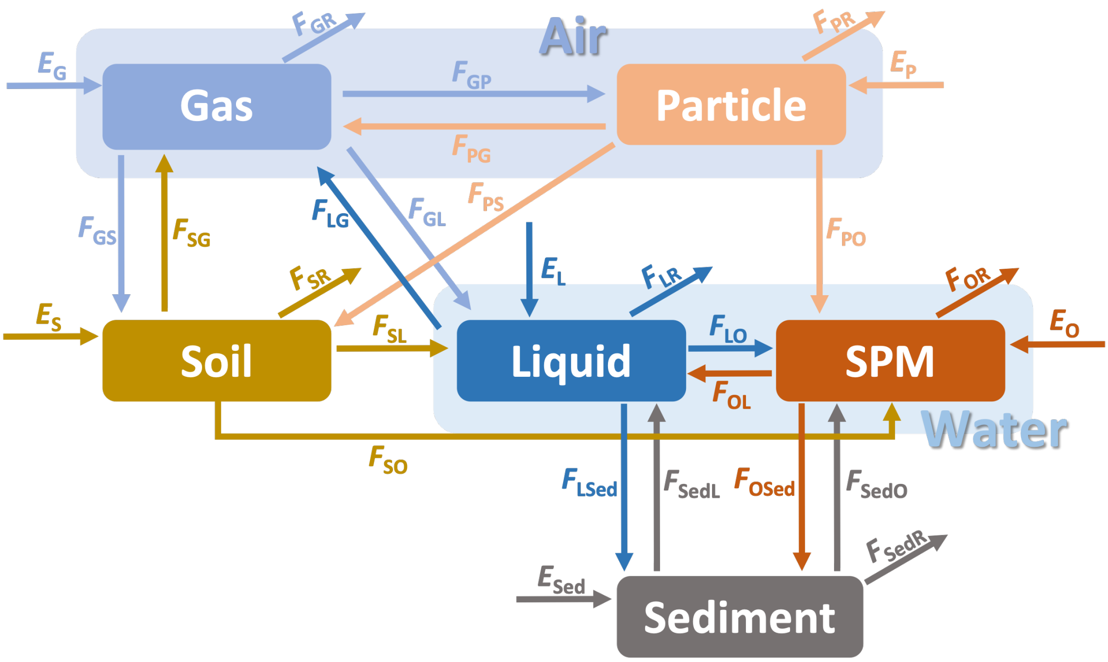

The six-compartment six-fugacity system

(Notes: E_i is the emission rate (mol/h) to compartment i; F_{ij} is the flux from compartment i to compartment j (mol/h); F_{iR} is the flux by reaction (mol/h); Particle represents particle in air; SPM represents suspended particle matter in water.)

The relationships between the above figure (focusing on the processes related to the six compartments) in Supporting Information and Fig.1 (focusing on the processes related to gas and particle phases) in the main text of the manuscript were described in detail as follows. For the gas phase, in the above figure, the flux of F_{GS} (flux from gas to soil) includes the diffusion flux from gas to soil (F_{GS_diff}) and the wet deposition flux from gas to soil (F_{GS_W}). The flux of F_{GL} (flux from gas to liquid) includes the diffusion flux from gas to soil (F_{GW_diff}) and the wet deposition flux from gas to liquid (F_{GW_W}). In the Fig. 1, the corresponding flux F_{GSW_diff} is the sum of F_{GS_diff} and F_{GW_diff}. F_{GW} is the sum of F_{GS_W} and F_{GW_W}. For the particle phase, in the above figure, the flux of F_{PO} (flux from particle to SPMs) includes wet deposition flux from particle to SPMs (F_{PO_W}) and dry deposition flux from particle to SPMs (F_{PO_D}). The flux of F_{PS} (flux from particle to soil) includes wet deposition flux from particle to soil (F_{PS_W}) and dry deposition flux from particle to soil (F_{PS_D}). In the Fig. 1, the corresponding flux F_{PD} is the sum of F_{PO_D} and F_{PS_D}. The flux F_{PW} is the sum of F_{PO_W} and F_{PS_W}.

Once the relationships between the six compartments were confirmed, the function between the total input flux and the total output flux can be established for each compartment. The relationship follows the general form:

$$E_{\mathrm{i}} + \sum D_{\mathrm{ji}} f_{\mathrm{j}} = \sum D_{\mathrm{ik}} f_{\mathrm{i}} + D_{\mathrm{iR}} f_{\mathrm{i}} \quad \text{(S2)}$$

where, E_i is the emission rate (mol/h) to compartment i; D_{ji} is the intermedia D values from compartment j to compartment i (mol/(Pa·h)); D_{ik} is the intermedia D values from compartment i to compartment k (mol/(Pa·h)); D_{iR} is the reaction rate D value in compartment i (mol/(Pa·h)); f_i and f_j are the fugacity of chemical in compartment i and compartment j (Pa).

In the present study, both the gaseous and particulate emissions were considered in the models. Therefore, the above equation for each compartment can be expressed as follows in detail:

Air: Gas phase:

$$E_{\mathrm{G}} + D_{\mathrm{LG}}f_{\mathrm{L}} + D_{\mathrm{SG}}f_{\mathrm{S}} + D_{\mathrm{PG}}f_{\mathrm{P}} = (D_{\mathrm{GL}} + D_{\mathrm{GS}} + D_{\mathrm{GP}} + D_{\mathrm{G}R})f_{\mathrm{G}} \quad \text{(S3)}$$

Air: Particle phase:

$$E_{\mathrm{P}} + D_{\mathrm{GP}}f_{\mathrm{G}} = (D_{\mathrm{PG}} + D_{\mathrm{PS}} + D_{\mathrm{PO}} + D_{\mathrm{P}R})f_{\mathrm{P}} \quad \text{(S4)}$$

Water: Dissolved phase:

$$D_{\mathrm{GL}}f_{\mathrm{G}} + D_{\mathrm{SL}}f_{\mathrm{S}} + D_{\mathrm{SedL}}f_{\mathrm{Sed}} + D_{\mathrm{OL}}f_{\mathrm{O}} = (D_{\mathrm{LG}} + D_{\mathrm{LSed}} + D_{\mathrm{LO}} + D_{\mathrm{L}R})f_{\mathrm{L}} \quad \text{(S5)}$$

Water: Solid phase:

$$D_{\mathrm{LO}}f_{\mathrm{L}} + D_{\mathrm{SO}}f_{\mathrm{S}} + D_{\mathrm{SedO}}f_{\mathrm{Sed}} + D_{\mathrm{PO}}f_{\mathrm{P}} = (D_{\mathrm{OL}} + D_{\mathrm{OSed}} + D_{\mathrm{O}R})f_{\mathrm{O}} \quad \text{(S6)}$$

Soil phase:

$$D_{\mathrm{GS}}f_{\mathrm{G}} + D_{\mathrm{PS}}f_{\mathrm{P}} = (D_{\mathrm{SG}} + D_{\mathrm{SL}} + D_{\mathrm{SO}} + D_{\mathrm{S}R})f_{\mathrm{S}} \quad \text{(S7)}$$

Sediment phase:

$$D_{\mathrm{LSed}}f_{\mathrm{S}} + D_{\mathrm{OSed}}f_{\mathrm{O}} = (D_{\mathrm{SedL}} + D_{\mathrm{SedO}} + D_{\mathrm{Sed}R})f_{\mathrm{Sed}} \quad \text{(S8)}$$

where *D* values for each intermedia process were given in **Table S1**.

The fugacity capacity *Z* values of each compartment used for calculation of the *D* values can be obtained by the equations in **Table S2**. The parameters for PAHs and environment were given in **Tables S3, S4 S5 and S6**. In the present study, the unit of the system was assumed as a cuboid with the air surface area (A_{A}) of 1 m^2, water surface area (A_{W}) of 0.7 m^2, and soil surface area (A_{S}) of 0.3 m^2. The height and/or depth of air, water and soil are 1000, 10 and 0.15 m, respectively.

The fugacity for each compartment can be obtained by analyzing the above equations. Then the parameters of each compartment and the parameters between different compartments can be calculated, such as fluxes, concentrations, mass fractions, and partitioning behavior (Qin et al., 2021; Li et al., 2021b; Li et al., 2021a).

Text S2. The calculation method of the output and input fluxes for the particle phase and the gas phase compartments

The 11 output and input fluxes for the particle phase and the gas phase can be calculated by the following equations:

$$(1-\phi_0)E = E_{\mathrm{G}} \tag{S9}$$

$$\phi_0 E = E_{\mathrm{P}} \tag{S10}$$

$$F_{GP} = D_{GP} f_G \tag{S11}$$

$$F_{\mathrm{PG}} = D_{\mathrm{GP}} f_{\mathrm{P}} \tag{S12}$$

$$F_{\mathrm{Gdiff}} = (D_{\mathrm{GDL}} + D_{\mathrm{GDS}}) f_{\mathrm{G}} \tag{S13}$$

$$F_{\mathrm{GW}} = (D_{\mathrm{GWL}} + D_{\mathrm{GWS}}) f_{\mathrm{G}} \tag{S14}$$

$$F_{\mathrm{diffG}} = D_{\mathrm{LG}} f_{\mathrm{L}} + D_{\mathrm{SG}} f_{\mathrm{S}} \tag{S15}$$

$$F_{\mathrm{PD}} = (D_{\mathrm{PDO}} + D_{\mathrm{PDS}}) f_{\mathrm{P}} = D_{\mathrm{PD}} f_{\mathrm{P}} \tag{S16}$$

$$F_{\mathrm{PW}} = (D_{\mathrm{PWO}} + D_{\mathrm{PWS}}) f_{\mathrm{P}} = D_{\mathrm{PW}} f_{\mathrm{P}} \tag{S17}$$

$$F_{\mathrm{GR}} = D_{\mathrm{GR}} f_{\mathrm{G}} \tag{S18}$$

$$F_{\mathrm{PR}} = D_{\mathrm{PR}} f_{\mathrm{P}} \tag{S19}$$

where the *D* values can be found in **Table S1**.

Text S3. The expression of the log K_P using fugacity method

The G–P partitioning coefficient (K_P) can be calculated as follows:

$$K_{\mathrm{P}} = (C_{\mathrm{P}}/C_{\mathrm{G}})/TSP \quad \text{(S20)}$$

where C_P (ng/m^3 air) and C_G (ng/m^3) are the PAHs concentrations in particle phase and gas phase, respectively, and TSP is the concentrations of total suspended particles (μg/m^3).

C_P can be transferred to C'_P (ng/m^3 particle) based the following equation:

$$C_{\mathrm{P}} = {C'}_{\mathrm{P}} \times TSP/10^9\rho_{\mathrm{P}} \quad \text{(S21)}$$

where C'_P (ng/m^3 particle) is the PAHs concentrations in particle phase with different units, and ρ_P is the density of particles (kg/m^3).

Then, the Eq. (S20) can be expressed in different form:

$$K_{\mathrm{P}} = ({C'}_{\mathrm{P}}/C_{\mathrm{G}})/10^9\rho_P \quad \text{(S22)}$$

The ratio of C'_P to C_G can be calculated using the method from the multimedia fugacity model:

$${C'}_{\mathrm{P}}/C_{\mathrm{G}} = f_{\mathrm{P}}Z_{\mathrm{P}}/f_{\mathrm{G}}Z_{\mathrm{G}} \quad \text{(S23)}$$

where Z_P/Z_G equal to K_{PG} at equilibrium state, which can be calculated by the following equation (Li et al., 2015):

$$K_{\mathrm{PG}} = Z_{\mathrm{P}}/Z_{\mathrm{G}} = 10^9\rho_P K_{\mathrm{P-HB}} \quad \text{(S24)}$$

where $K_{P\text{-}HB}$ is the G–P partitioning coefficient calculated from the H-B model (the equilibrium-state model) (Harner and Bidleman, 1998b).

Summarizing the equations above, log K_P can be expressed as following equation:

$$\log K_{\mathrm{P}} = \log K_{\mathrm{P-HB}} + \log(f_{\mathrm{P}}/f_{\mathrm{G}}) \quad \text{(S25)}$$

Text S4. The introduction of the prediction models

The H-B model

Under assumptions that the dominate G–P distribution process was absorption and the system was in *equilibrium-state*, an equation (named as the *H-B* model in the present study) used to predict the value of K_P for SVOCs was derived in an early study (Harner and Bidleman 1998b)

$$\log K_{\mathrm{P-HB}} = \log K_{\mathrm{OA}} + \log f_{\mathrm{OM}} - 11.91 \quad \text{(S26)}$$

The L-M-Y model

Li et al. established a *steady-state* model (named as the *L-M-Y* model in the present study) for the investigation of the G–P partitioning behavior of PBDEs (Li et al. 2015). The influences of dry and wet depositions of particles on the G–P partitioning were considered in the *L-M-Y* model. A non-equilibrium parameter caused by dry and wet depositions of particles, $\log \alpha$ was introduced into the *L-M-Y* model:

$$\log K_{\mathrm{P-LMY}} = \log K_{\mathrm{P-HB}} + \log \alpha \quad \text{(S27)}$$

$$\log \alpha = -\log(1 + 4.18 \times 10^{-11} f_{\mathrm{OM}} K_{\mathrm{OA}}) \quad \text{(S28)}$$

Therefore, the *H-B* model is a special case of the *L-M-Y* model when the non-equilibrium term ($\log \alpha$) equal zero.

Text S5. The calculation method of the root mean square error

To evaluate the performance of the new steady-state model, the root mean square error (RMSE) was calculated based on the following equation:

$$RMSE = \sqrt{\frac{1}{n}\sum(\log K_{\mathrm{P-P}} - \log K_{\mathrm{P}})^2} \qquad \text{(S29)}$$

where $\log K_{\mathrm{P\text{-}P}}$ is the prediction data from the new steady-state model, and $\log K_{\mathrm{P}}$ is the monitored data.

The smaller of the RMSE value indicated the better matching degree between the predicted data and the monitored data.

S2. Tables

Table S1 The transport parameter D (mol/(Pa·h)) for the multimedia fugacity model

Compartments	Symbol	D values	Process
Gas-Liquid	D_{GDL}	$1/[1/(k_{VG}A_{12}Z_G)+1/(k_{VW}A_{12}Z_W)]$	Diffusion
	D_{GWL}	$A_{12}U_RZ_W$	Rain dissolution
	D_{GL}	$D_{GDL}+D_{GWL}$	Gas → Liquid
	D_{LG}	D_{GDL}	Liquid → Gas
Gas-Soil	D_{GDS}	$1/[1/(k_{EG}A_{13}Z_G)+Y_3/[A_{13}(B_{MG}Z_G+B_{MW}Z_W)]]$	Diffusion
	D_{GWS}	$A_{13}U_RZ_W$	Rain dissolution
	D_{GS}	$D_{GDS}+D_{GWS}$	Gas → Soil
	D_{SG}	D_{GDS}	Soil → Gas
Particles-SPMs	D_{PWO}	$A_{12}U_RQ\upsilon_PZ_P$	Wet deposition
	D_{PDO}	$A_{12}U_D\upsilon_PZ_P$	Dry deposition
	D_{PO}	$D_{PWO}+D_{PDO}$	Particle → SPMs
Particles-Soil	D_{PWS}	$A_{13}U_RQ\upsilon_PZ_P$	Wet deposition
	D_{PDS}	$A_{13}U_D\upsilon_PZ_P$	Dry deposition
	D_{PS}	$D_{PWS}+D_{PDS}$	Particle → Soil
Gas-Particles	D_{PG}	$A_Pk_{PG}Z_G$	Sorption and desorption
	D_{GP}	D_{PG}	Gas → Particle
	D_{PG}	D_{PG}	Particle→Gas
Soil-Liquid	D_{SL}	$A_{13}U_{WW}Z_W$	Water runoff
	D_{SL}	D_{SL}	Soil → Liquid
Soil-SPMs	D_{SO}	$A_{13}U_{EW}Z_S$	Soil runoff
	D_{SO}	D_{SO}	Soil → SPM
Liquid-SPMs	D_{LO}	$A_Ok_{WO}Z_W$	Sorption and desorption

Compartments	Symbol	*D* values	Process
Sediment-Liquid	D_{LO}	D_{LO}	Liquid → SPMs
	D_{OL}	D_{LO}	SPMs → Liquid
	D_{SedL}	$1/[1/(k_{SW}A_{24}Z_W)+Y_4/(B_{MW}A_{24}Z_W)]$	diffusion
	D_{SedL}	D_{SedL}	Liquid → Sediment
	D_{LSed}	D_{SedL}	Sediment → Liquid
Sediment-SPMs	D_{OSed}	$U_{DO}A_{24}Z_O$	Deposition
	D_{SedO}	$U_{RS}A_{24}Z_{Sed}$	Resuspension
	D_{OSed}	D_{OSed}	SPMs → Sediment
	D_{SedO}	D_{SedO}	Sediment → SPMs
Degradation	D_{iR}	$k_{degi}V_iZ_i$	Degradation in compartment i

Notes: The gaseous degradation rate of PAHs can be calculated using the half-lives of PAHs: $k_{degi} = \ln(2)/t_{1/2}$ (The half-lives of the 15 PAHs can be found in **Table S5**).

Table S2. The fugacity capacity *Z* values and the partition parameter *K* values for the multimedia fugacity model

Z	Equation	Unit
Z_G	$1/RT$	mol/(m^3·Pa)
Z_W	$1/H$ or Z_G/K_{AW}	mol/(m^3·Pa)
Z_S	$K_{SG}Z_G$	mol/(m^3·Pa)
Z_{sed}	$K_{SedW}Z_W$	mol/(m^3·Pa)
Z_P	$K_{PG}Z_G$	mol/(m^3·Pa)
Z_O	$K_{PW}Z_W$	mol/(m^3·Pa)

Table S3. The partition parameter *K* values for the multimedia fugacity model

K Process	*K*	Equation	Unit
Soil-Gas	K_{SG}	$f_{OM(S)}K_{OA}$	dimensionless
Sediment-Liquid	K_{SedW}	$f_{OC(Sed)}K_{OC}\rho_{Sed}/1000$	dimensionless
Gas-Particle	K_{PG}	$10^{-2.91}\rho_P f_{OM}K_{OA}$	dimensionless
SPMs-Liquid	K_{PW}	$f_{OC(O)}\rho_O K_{OC}/1000$	dimensionless
Organic carbon-Water	K_{OC}	$0.41(L/kg)K_{OW}$	L/kg
Air-Water	K_{AW}	$\log K_{AW} = A_{AW} + B_{AW} / T_W$	dimensionless
Octanol-Water	K_{OW}	$\log K_{OW} = A_{OW} + B_{OW} / T_W$	dimensionless
Octanol-Air	K_{OA}	$\log K_{OA} = A_{OA} + B_{OA} / T$	dimensionless

Note: T and T_W are the temperature in atmosphere and in water, respectively, K; The values of T equal to T_W when the temperature in air higher than 0°C, and the value of T_W equal to the constant value when the temperature in air lower than 0°C; The values of A and B for the calculation of K_{AW}, K_{OW}, K_{OA} can be calculated (See details in **Table S4**).

Table S4. The values of *A* and *B* for the PAHs

PAHs	Abbreviations	A_{AW}	B_{AW}	A_{OW}	B_{OW}	A_{OA}	B_{OA}
acenaphthylene	Acy	5.46	−2272	1.67	593	−1.97	2476
acenaphthene	Ace	5.66	−2251	1.43	774	−2.20	2597
fluorene	Flu	5.97	−2483	1.56	816	−2.61	2833
phenanthrene	Phe	6.06	−2607	1.49	944	−3.37	3293
anthracene	Ant	6.14	−2620	1.73	867	−3.41	3316
fluoranthene	Fluo	6.44	−2850	0.83	1295	−4.34	3904
pyrene	Pyr	6.29	−2780	1.09	1182	−4.56	3985
benzo[a]anthracene	BaA	7.10	−3222	0.99	1453	−5.64	4746
chrysene	Chr	7.01	−3205	0.91	1499	−5.65	4754
benzo[b]fluoranthene	BbF	7.39	−3438	−0.33	1847	−6.40	5285
benzo[k]fluoranthene	BkF	7.47	−3458	0.10	1870	−6.42	5301
benzo[a]pyrene	BaP	7.25	−3374	0.32	1709	−6.50	5382
indeo[1,2,3-cd]pyrene	IcdP	7.63	−3614	−0.73	2177	−7.00	5791
dibenzo[a,h]anthracene	DahA	7.97	−3805	0.52	1986	−7.17	5887
benzo[g.h,j]perylene	BghiP	7.41	−3526	−0.67	2245	−7.03	5834

Note: The values of A_{OA} and B_{OA} were cited from references (Odabasi et al., 2006; Harner and Bidleman, 1998a), except the values for Nap were calculated by the equations: $B_X = U_X/(\ln(10)*8.314)$, $A_X = \log K_X(25°C) - B_X/298.15$ (X represent AW, OW, and OA). A_{OW} and B_{OW} were also calculated using the above equations. The values in the equations (log K_X, U_X) were calculated using the UFZ - LSER Database (https://www.ufz.de/index.php?en=31698&contentonly=1&m=0&lserd_data[mvc]=Public/start). A_{AW} and B_{AW} were calculated by the equations: $A_{AW} = A_H - 3.351$, $B_{AW} = B_H$ (A_H and B_H were parameters used for the calculation of the Henry's Law constants (Parnis et al., 2016), $\log K_{AW} = \log H - \log (R*T)$, $\log (R*T) \approx 3.351$ when temperature ranged from 223 K to 323 K). log K_{OW} (25°C) for BbF and IcdP were cited from the reference (Ma et al., 2010). U_{OW} for BbF and IcdP were calculated from $U_{OW} = U_{OA} + U_{AW}$.

Table S5. The half-lives of 15 PAHs in different phases (h^{-1})

PAHs	t_A	t_W	t_S	t_{Sed}	t_P	t_O
Acy	1.70	360	7.20×10^2	3.24×10^3	7.20×10^2	3.24×10^3
Ace	1.92	900	1.80×10^3	8.10×10^3	1.80×10^3	8.10×10^3
Flu	14.5	360	7.20×10^2	3.24×10^3	7.20×10^2	3.24×10^3
Phe	9.87	1440	2.88×10^3	1.30×10^4	2.88×10^3	1.30×10^4
Ant	3.21	1440	2.88×10^3	1.30×10^4	2.88×10^3	1.30×10^4
Fluo	4.39	1440	2.88×10^3	1.30×10^4	2.88×10^3	1.30×10^4
Pyr	2.57	1440	2.88×10^3	1.30×10^4	2.88×10^3	1.30×10^4
BaA	2.57	1440	2.88×10^3	1.30×10^4	2.88×10^3	1.30×10^4
Chr	2.57	1440	2.88×10^3	1.30×10^4	2.88×10^3	1.30×10^4
BbF	6.92	1440	2.88×10^3	1.30×10^4	2.88×10^3	1.30×10^4
BkF	2.39	1440	2.88×10^3	1.30×10^4	2.88×10^3	1.30×10^4
BaP	2.57	1440	2.88×10^3	1.30×10^4	2.88×10^3	1.30×10^4
IcdP	1.99	1440	2.88×10^3	1.30×10^4	2.88×10^3	1.30×10^4
DahA	2.57	1440	2.88×10^3	1.30×10^4	2.88×10^3	1.30×10^4
BghiP	1.48	1440	2.88×10^3	1.30×10^4	2.88×10^3	1.30×10^4

Note: The data were cited from the Estimation Programs Interface (EPI) Suite ™ (the US Environmental Protection Agency's Office of Pollution Prevention and Toxics and Syracuse Research Corporation (SRC)).

Table S6. The environmental parameters for the multimedia fugacity model

Parameters	Description	Value	Unit	Function
k_{VG}	Gas side MTC over water	3	m/h	
k_{VW}	Liquid side MTC	0.03	m/h	
U_R	Rainfall rate	9.70×10^{-5}	m/h	
Q	Scavenging ratio	2×10^{5}	–	
v_P	Volume fraction of aerosol particle	6.67×10^{-11}	–	$10^{-9}TSP/\rho_P$
U_D	Dry deposition velocity	10.8	m/h	
k_{EG}	Gas side MTC over soil	1	m/h	
Y_3	Diffusion path length in soil	0.05	m	
B_{MG}	Molecular diffusivity in gas	0.04	m^2/h	
B_{MW}	Molecular diffusivity in liquid	4.00×10^{-6}	m^2/h	
U_{WW}	Liquid runoff rate from soil	3.90×10^{-5}	m/h	
U_{EW}	Solids runoff rate from soil	2.30×10^{-8}	m/h	
k_{SW}	Liquid side MTC over sediment	0.01	m/h	
Y_4	Diffusion path length in sediment	0.005	m	
U_{DO}	SPMs deposition rate	4.60×10^{-8}	m/h	
U_{RS}	Sediment resuspension rate	1.10×10^{-8}	m/h	
k_{PG}	Gas-Particle Partitioning MTC	1.89×10^{1}	m/h	$C\ B_{PG}/l_{PG}$
B_{PG}	Molecular diffusivity in air	1.80×10^{-2}	m^2/h	
l_{PG}	Air boundary layer thickness	4.75×10^{-3}	m	
C	Accommodation coefficient	5	–	
k_{WO}	Solid-Dissolved Partitioning MTC	4.21×10^{-3}	m/h	$C'\ B_{WO}/l_{WO}$
B_{WO}	Molecular diffusivity in water	4.00×10^{-6}	m^2/h	
l_{WO}	Water boundary layer thickness	4.75×10^{-3}	m	
C'	Accommodation coefficient	5	–	
$\rho_P/\rho_O/\rho_{Sed}$	Density of particles in air and water and sediment	1.50×10^{3}	kg/m^3	
d_P/d_O	Diameter of particles in air and water	1.00×10^{-7}	m	
TSP	Concentration of particles in air	1.00×10^{2}	ug/m^3	
SPM	Concentration of particles in water	10	g/m^3	

continued Table S6

Parameters	Description	Value	Unit	Function
$f_{OC(O)}$	Fraction of organic carbon in SPMs	0.04	–	
$f_{OM(S)}$	Fraction of organic materials in soil	0.04	–	
$f_{OC(Sed)}$	Fraction of organic carbon in sediment	0.1	–	
A_P	Total area of particles in air	4	m^2	$6\times10^{-9} TSP\times V_G/(\rho_P d_P)$
A_O	Total area of particles in Water	2800	m^2	$6\times10^{-3} SPM\times V_W/(\rho_O d_O)$

Note: The values of the parameters were cited from Mackay (2001) (Mackay, 2001).

S3. Figures

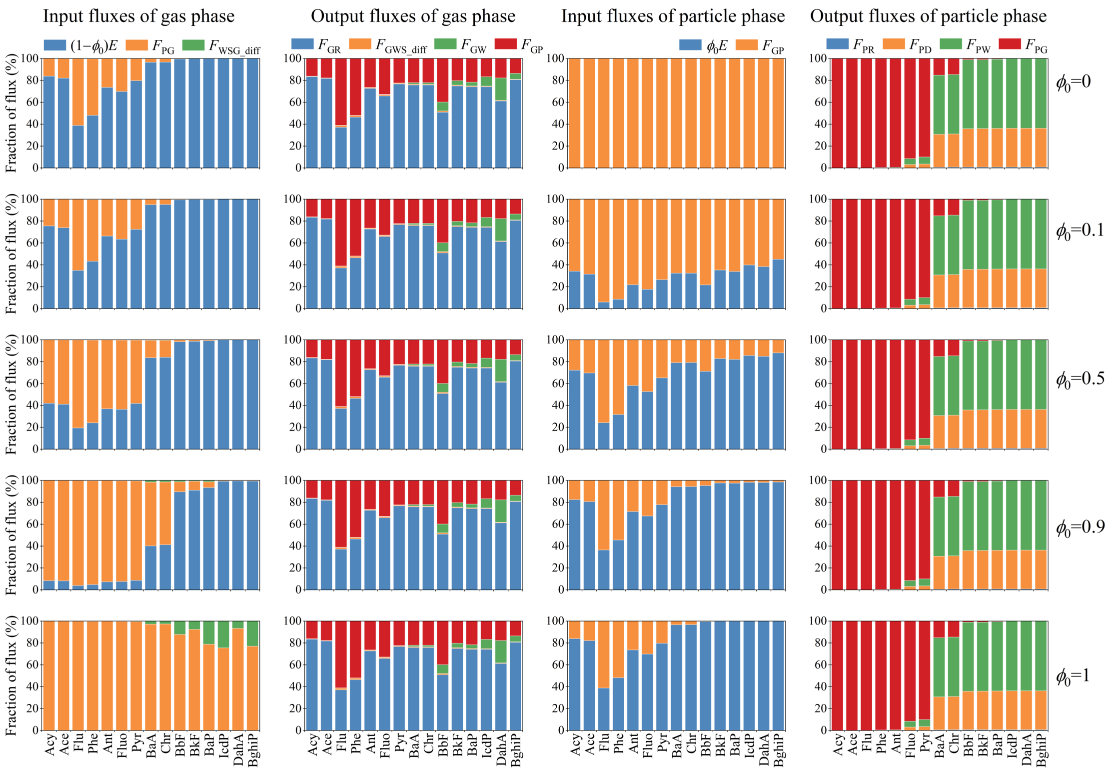

Fig. S1. Comparison of the fluxes for the input and output fluxes of the gas phase and particle phase

Note: F_{GR}: degradation flux of gas phase PAHs; F_{PR}: degradation flux of particle phase PAHs; F_{GP}: migration flux from gas phase to particle phase; F_{PG}: migration flux from particle phase to gas phase; F_{GWS_diff}: diffusion fluxes from gas phase to water and soil phases; F_{GW}: wet deposition flux of gas phase PAHs; F_{WSG_diff}: diffusion fluxes from soil and water phases to gas phase; F_{PD}: dry deposition flux of particle phase PAHs; F_{PW}: wet deposition flux of particle phase PAHs; $(1-\phi_0)E$: emission flux of gas phase PAHs; $\phi_0 E$: emission flux of particle phase PAHs.

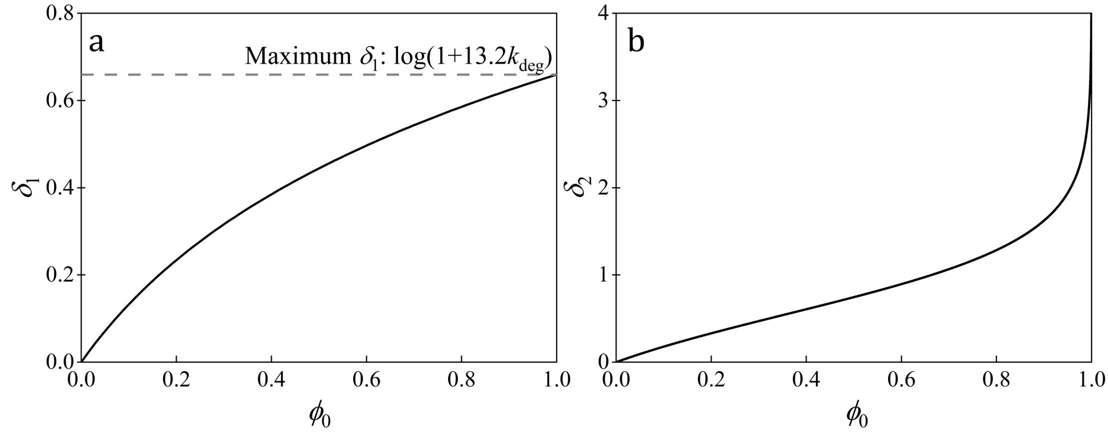

Fig. S2. The difference between the new steady-state model with the H-B model and the L-M-Y model

Note: δ_1 and δ_2 were calculated based on the value of k_{deg} = 0.27 h^{-1}, δ_1 is the difference between the new steady-state model with the H-B model and the L-M-Y model when log K_{OA} < log K_{OA1}, and δ_2 is the difference between the new steady-state model with the L-M-Y model when log K_{OA} > log K_{OA2}.

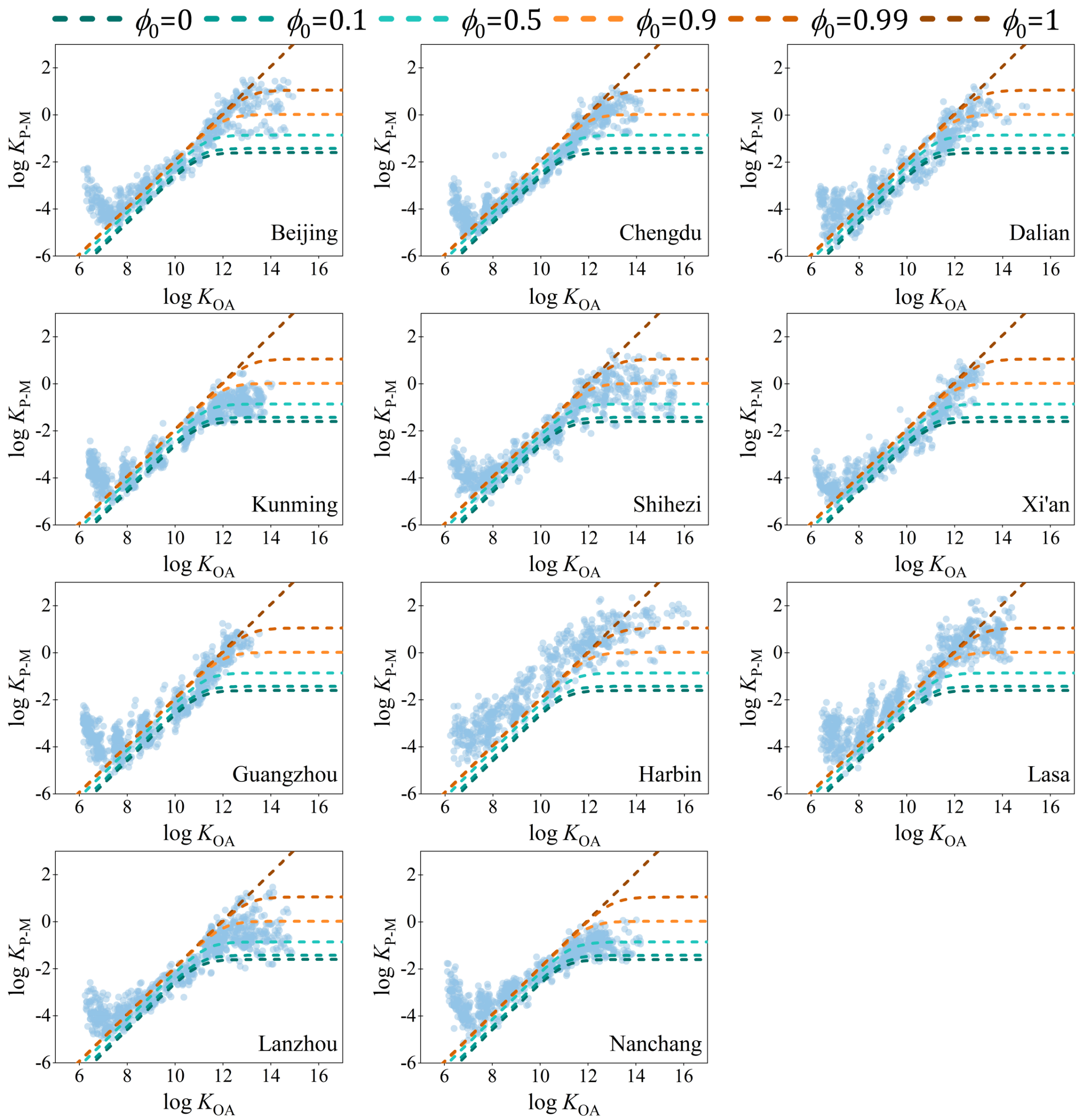

Fig. S3. The comparison between the monitored data of log $K_{P\text{-}M}$ of PAHs from 11 cities in China and the prediction lines of the new steady-state model with different values of ϕ_0.

Note: the k_{deg} of 0.27 h^{-1} and f_{OM} of 0.21 were used in the new steady-state model.

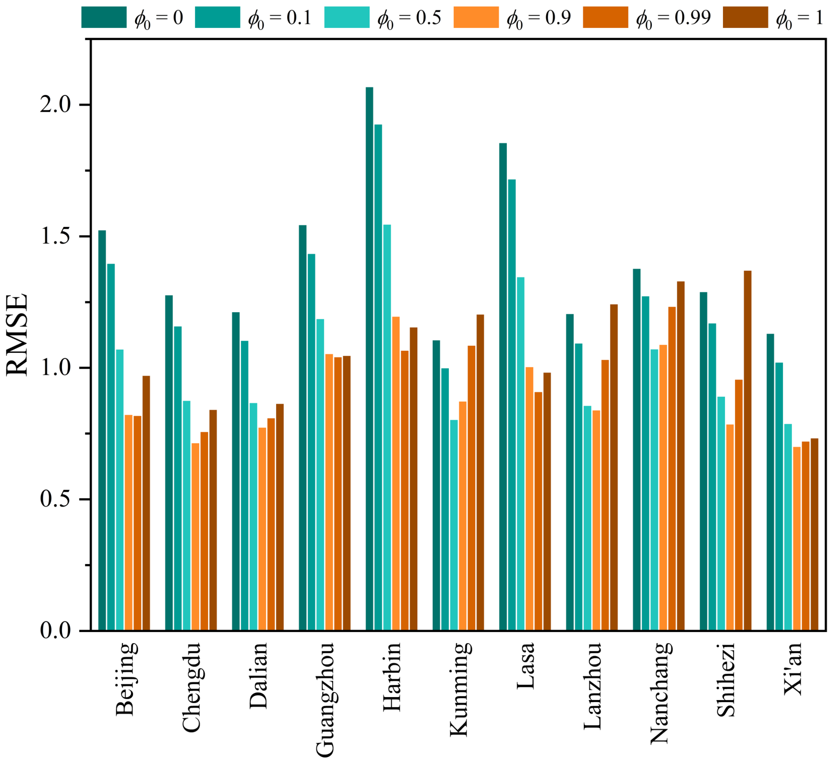

Fig. S4. The values of RMSE for the new steady-state model based on the monitored data from 11 cities in China

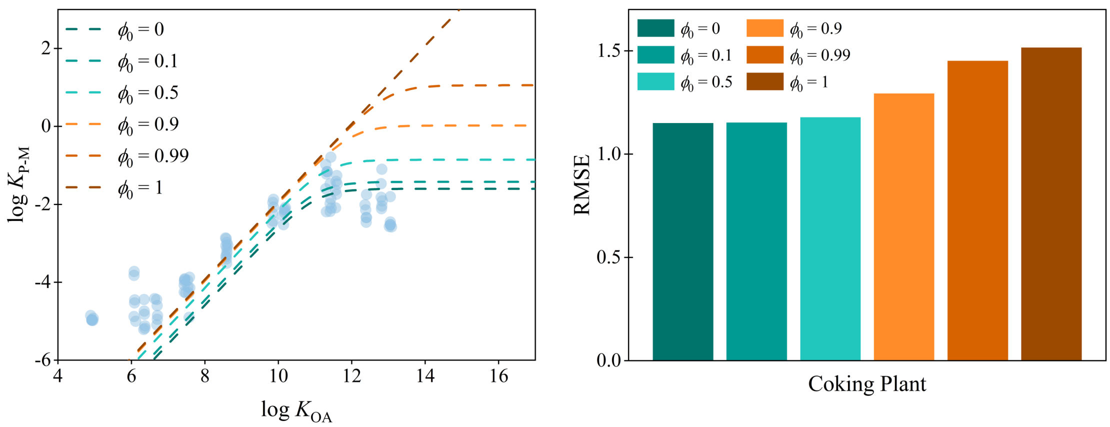

Fig. S5. The comparison between the monitored data of log $K_{P\text{-}M}$ of PAHs from a coking plant and the prediction lines of the new steady-state model with different values of ϕ_0 (left panel) and the related values of RMSE of the new steady-state model (right panel)

Note: The k_{deg} of 0.27 h^{-1} and f_{OM} of 0.21 were used in the new steady-state model; and the monitored data were cited from a coking plant (Liu et al., 2019).

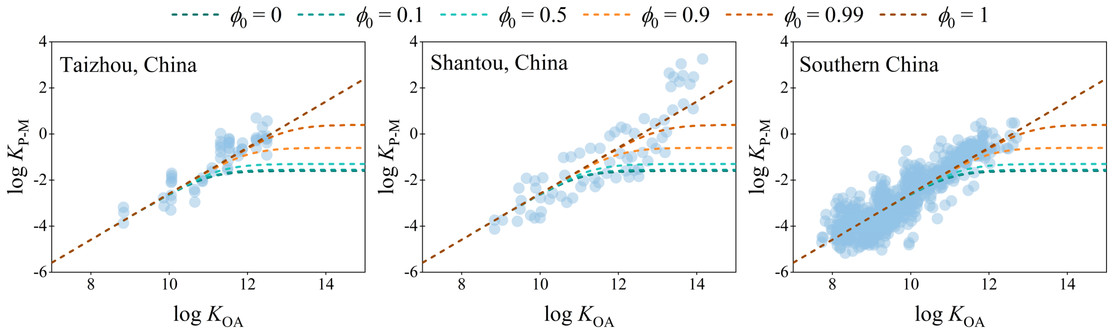

Fig. S6. The comparison between the monitored data of log $K_{P\text{-}M}$ of PBDEs from E-waste sites and the prediction lines of the new steady-state model with different values of ϕ_0

Note: The k_{deg} of 0.27 h^{-1} and f_{OM} of 0.21 were used in the new steady-state model; and the monitored data were cited from the following references: Taizhou, China (Han et al., 2009); Shantou, China (Chen et al., 2011); and Southern China (Tian et al., 2011).

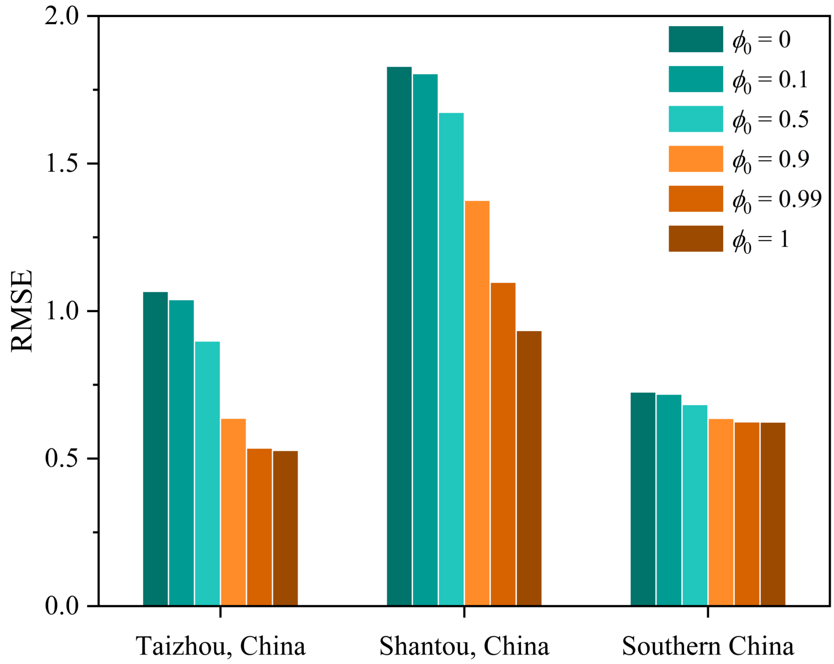

Fig. S7. The values of the RMSE of the new steady-state model based on the monitored data of PBDEs from e-waste sites

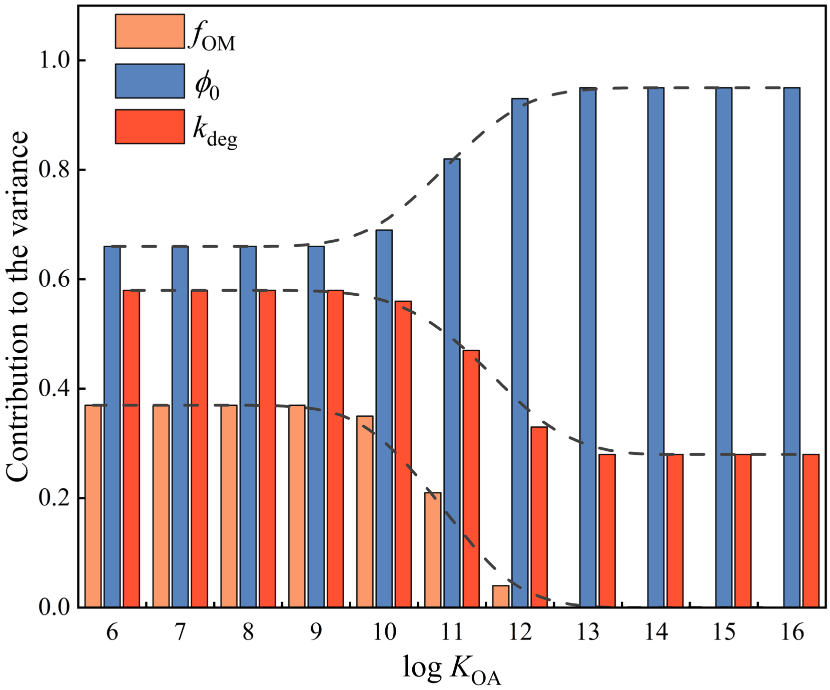

Fig. S8. Sensitivity analysis for the parameters of ϕ_0, f_{OM}, and k_{deg} in the new steady-state model

Note: Sensitivity analysis was conducted by the Monte Carlo analysis with 100,000 trials using the commercial software package Oracle Crystal Ball. The following variables with their distribution patterns and confidence factors (CF) were considered: ϕ_0: uniform distribution, 0 to 1; f_{OM}, lognormal distribution, mean = 0.21, CF = 1.5 (Mackay, 2001); k_{deg}, lognormal distribution, mean = 0.27, CF = 3 (Wania and Dugani, 2003).

References

Chen, D., Bi, X., Liu, M., Huang, B., Sheng, G., and Fu, J.: Phase partitioning, concentration variation and risk assessment of polybrominated diphenyl ethers (PBDEs) in the atmosphere of an e-waste recycling site, Chemosphere, 82, 1246-1252, https://doi.org/10.1016/j.chemosphere.2010.12.035, 2011.

Han, W., Feng, J., Gu, Z., Chen, D., Wu, M., and Fu, J.: Polybrominated Diphenyl Ethers in the Atmosphere of Taizhou, a Major E-Waste Dismantling Area in China, Bul. Environ. Contam. Toxicol., 83, 783-788, https://doi.org/10.1007/s00128-009-9855-9, 2009.

Harner, T. and Bidleman, T. F.: Measurement of Octanol−Air Partition Coefficients for Polycyclic Aromatic Hydrocarbons and Polychlorinated Naphthalenes, Journal of Chemical & Engineering Data, 43, 40-46, http://doi.org/10.1021/je970175x, 1998a.

Harner, T. and Bidleman, T. F.: Octanol-air partition coefficient for describing particle/gas partitioning of aromatic compounds in urban air, Environ. Sci. Technol., 32, 1494-1502, https://doi.org/10.1021/es970890r, 1998b.

Li, Y., Ma, W., and Yang, M.: Prediction of gas/particle partitioning of polybrominated diphenyl ethers (PBDEs) in global air: A theoretical study, Atmospheric Chemistry and Physics, 15, 1669-1681, https://doi.org/10.5194/acp-15-1669-2015, 2015.

Li, Y.-F., Qin, M., Yang, P.-F., Hao, S., and Macdonald, R. W.: Particle/gas partitioning for semi-volatile organic compounds (SVOCs) in Level III multimedia fugacity models: Gaseous emissions, Sci. Total Environ., 795, 148729, https://doi.org/10.1016/j.scitotenv.2021.148729, 2021a.

Li, Y.-F., Qin, M., Yang, P.-F., Liu, L.-Y., Zhou, L.-J., Liu, J.-N., Shi, L.-L., Qiao, L.-N., Hu, P.-T., Tian, C.-G., Nikolaev, A., and Macdonald, R.: Treatment of particle/gas partitioning using level III fugacity models in a six-compartment system, Chemosphere, 271, 129580, https://doi.org/10.1016/j.chemosphere.2021.129580, 2021b.

Liu, X., Zhao, D., Peng, L., Bai, H., Zhang, D., and Mu, L.: Gas–particle partition and spatial characteristics of polycyclic aromatic hydrocarbons in ambient air of a prototype coking plant, Atmos. Environ., 204, 32-42, https://doi.org/10.1016/j.atmosenv.2019.02.012, 2019.

Ma, Y.-G., Lei, Y. D., Xiao, H., Wania, F., and Wang, W.-H.: Critical Review and Recommended Values for the Physical-Chemical Property Data of 15 Polycyclic Aromatic Hydrocarbons at 25 degrees C, J. Chem. Eng. Data, 55, 819-825, http://doi.org/10.1021/je900477x, 2010.

Mackay, D.: Multimedia Environmental Models: the Fugacity Approach, Taylor & Francis, New York, 2001.

Odabasi, M., Cetin, E., and Sofuoglu, A.: Determination of octanol-air partition coefficients and supercooled liquid vapor pressures of PAHs as a function of temperature: Application to gas-particle partitioning in an urban atmosphere, Atmos. Environ., 40, 6615-6625, http://doi.org/10.1016/j.atmosenv.2006.05.051, 2006.

Parnis, J. M., Mackay, D., and Harner, T.: Temperature dependence of Henry's law constants and K-OA for simple and heteroatom-substituted PAHs by COSMO-RS (vol 110, pg 27, 2015), Atmos. Environ., 136, 21-21, http://doi.org/10.1016/j.atmosenv.2016.04.009, 2016.

Qin, M., Yang, P., Hu, P., Hao, S., Macdonald, R. W., and Li, Y.: Particle/gas partitioning for semi-volatile organic compounds (SVOCs) in level III multimedia fugacity models: Both gaseous and particulate emissions, Sci. Total Environ., 790, 148012, https://doi.org/10.1016/j.scitotenv.2021.148012, 2021.

Tian, M., Chen, S.-J., Wang, J., Zheng, X.-B., Luo, X.-J., and Mai, B.-X.: Brominated Flame Retardants in the Atmosphere of E-Waste and Rural Sites in Southern China: Seasonal Variation, Temperature Dependence, and Gas-Particle Partitioning, Environ. Sci. Technol., 45, 8819-8825, https://doi.org/10.1021/es202284p, 2011.

Wania, F. and Dugani, C. B.: Assessing the long-range transport potential of polybrominated diphenyl ethers: a comparison of four multimedia models, Environ. Toxicol. Chem., 22, 1252-1261, https://doi.org/10.1002/etc.5620220610, 2003.